

Local electronic structure in the Peyrard–Bishop–Holstein model

This article has been downloaded from IOPscience. Please scroll down to see the full text article.

2007 J. Phys.: Condens. Matter 19 136203

(<http://iopscience.iop.org/0953-8984/19/13/136203>)

View [the table of contents for this issue](#), or go to the [journal homepage](#) for more

Download details:

IP Address: 129.252.86.83

The article was downloaded on 28/05/2010 at 16:50

Please note that [terms and conditions apply](#).

Local electronic structure in the Peyrard–Bishop–Holstein model

Jian-Xin Zhu, K Ø Rasmussen, A V Balatsky and A R Bishop

Theoretical Division, Los Alamos National Laboratory, Los Alamos, NM 87545, USA

Received 12 January 2007, in final form 8 February 2007

Published 12 March 2007

Online at stacks.iop.org/JPhysCM/19/136203

Abstract

There is increasing evidence for polaronic effects on charge localization and dynamics in DNA. The Peyrard–Bishop–Holstein model has been previously suggested as an appropriate model for the description of such effects. Here we report a self-consistent study of local electronic structure within this model for both homopolymer and realistic viral P5 promoter segments. Our results indicate that both the inter-base-pair stacking interaction and the electron filling can qualitatively influence the polaronic properties in a specific DNA sequence, including features of two distinct length scales and competition with sequence-disorder induced localization.

(Some figures in this article are in colour only in the electronic version)

There has been heightened interest in recent years in the electronic aspects of DNA, particularly regarding charge storage, localization and dynamics (for a review see [1–3]). This interest is driven both by biological considerations (e.g., replication, damage, repair mechanisms) [4, 5] and also by attempts to use the reproducibility of the DNA structure for nanoscale device applications (sensors, transistors, etc) [6, 7]. Whilst the average (double-helix) structure of DNA is now a well-characterized structural template, it is increasingly evident that strong, local deviations from the average structure determine configurations which carry essential functionalities. An example is the formation of a ‘polaron’, in which an added charge induces a local structural distortion around the charge. For instance, polaron mechanisms for charge migration [5, 8–15], have been suggested in conductivity experiments on homopolymer DNA [16].

An essential embellishment of the simplest Holstein-type polaron follows from the recognition that the DNA double-helix structure is inherently ‘soft’. This feature is represented, through a nonlinear base-pair stacking interaction, in the Peyrard–Bishop (PB) model which has been introduced [17–20] to successfully describe both denaturation and transcription initiation sites for many DNA sequences. The coupling of charge with this nonlinear PB model, forming the Peyrard–Bishop–Holstein (PBH) model, goes much beyond the original Holstein model in solid state physics and should describe more accurately the coupled structural and electronic aspects of DNA. Within the PBH model, adding charges to soft DNA reveals novel polaronic

behaviour—both structurally and electronically. In previous studies [11, 13, 14], a single-body time-dependent Schrödinger equation was solved for the study of polaron dynamics, and no many-electron (i.e., Fermi statistics) effect were included. Also, a homopolymer DNA has been typically considered. On the other hand, the pioneering studies [21, 22] of coherent charge transport in both periodic and aperiodic DNA sequences have shown clearly the importance of characteristic sequence dependence. In the present work, we explore the local electronic structure in the static PBH model in both homopolymer and viral P5 promoter segments. The P5 sequence is studied as a well-characterized example of a real biological sequence to examine the effects of base-pair disorder on polaron formation and structure. We find that both the inter-base-pair stacking interaction and the electron filling can significantly affect the polaronic properties in a specific DNA sequence. In particular, we find the signatures of two principal length scales—a long-range ‘elastic’ scale accompanying a shorter polaronic one. The local electronic structure may be directly measured by local probes such as scanning tunnelling microscopy (STM), which has recently found application in the study of DNA [23].

We study a one-dimensional model of electrons having a Holstein-type coupling to the displacement field of the bases. The Hamiltonian of the whole system is given by

$$\mathcal{H} = \mathcal{H}_e + \mathcal{H}_{eb} + \mathcal{H}_b. \quad (1)$$

Here the first term represents the electron degrees of freedom without coupling:

$$\mathcal{H}_e = -t \sum_i (c_i^\dagger c_{i+1} + \text{H.c.}) + \sum_i \epsilon_i c_i^\dagger c_i, \quad (2)$$

where the c_i^\dagger (c_i) are electron creation (annihilation) operators on site i . The variables t and ϵ_i are the hopping integral between two nearest-neighbour base-pairs and the on-site potential energy, respectively. For simplicity, we consider the electrons to be spinless. The second term on the right-hand side (RHS) of equation (1) represents the coupling of the electronic degrees of freedom and base displacement field:

$$\mathcal{H}_{eb} = \alpha_v \sum_i y_i c_i^\dagger c_i, \quad (3)$$

where y_i denotes the displacement from the equilibrium position of the base-pairs. The variable α_v characterizes the coupling strength. The third term \mathcal{H}_b represents the displacement field of the bases of the double-stranded DNA. In the PB model for the displacement field, the most relevant degrees of freedom, namely the *transverse* stretching of the hydrogen bonds connecting complementary bases in the opposite strands of the double helix, are captured. In an adiabatic approximation, it is sufficient to consider the potential energy only such that

$$\mathcal{H}_b = \sum_i \left[D_i (e^{-a_i y_i} - 1)^2 + \frac{k_v}{2} (1 + \rho e^{-\alpha(y_i + y_{i-1})}) (y_i - y_{i-1})^2 \right]. \quad (4)$$

Here the Morse potential in the first term provides the effective interaction between complementary bases. It represents both the attraction due to the hydrogen bonds forming the base-pairs and the repulsion of the negatively charged phosphates in the backbone of the two strands screened by the surrounding solvent. The parameters D_i and a_i of the on-site potential distinguish between the two possible combinations of bases, i.e., adenine–thymine (AT) or guanine–cytosine (CG), at site i , depending on the particular sequence. The second term in the total potential energy represents the stacking interaction between adjacent base-pairs. Note that the nonlinear inter-site coupling, given by the exponential term that effectively modifies a harmonic spring constant, is essential for representing local constraints in nucleotide motions, which result in long-range cooperative ‘elasticity’ effects [18]. Physically, the constraint describes the change of the next-neighbour stacking interaction due to the distortion of the

hydrogen bonds connecting a base-pair, mediated through the redistribution of the electrons on the corresponding bases. Despite its reduced character (involving a small number of variables), it is more realistic than the harmonic model and has been successful in capturing important thermodynamic properties in various DNA chains [24–26], including denaturation and, even more notably, transcription initiation.

After performing a canonical transformation, the electronic part of the Hamiltonian $H_e + H_{eb}$ can be diagonalized by solving the equation

$$-t\phi_{i+1}^n - t\phi_{i-1}^n + (\epsilon_i + \alpha_v y_i)\phi_i^n = E_n \phi_i^n, \quad (5)$$

where ϕ_i^n and E_n are the n th eigenfunction and the corresponding eigenvalue, respectively. The self-consistency condition for y_i is given by

$$\left\langle \frac{\partial H_b}{\partial y_i} + \frac{\partial H_{eb}}{\partial y_i} \right\rangle = 0, \quad (6)$$

where the symbol $\langle \cdot \cdot \rangle$ represents the ensemble average over the electronic degrees of freedom. Specifically, at zero temperature, the average electron number per site appearing in $\langle H_{eb} \rangle$ is given by $n_i = \sum_{n=1}^{N_e} |\phi_i^n|^2$ with N_e the total number of electrons. To solve equations (5) and (6) self-consistently, an iteration method is used: given an initial distribution of $\{y_i\}$, we exactly diagonalize equation (5) to calculate the electron occupation on each site, $\langle n_i \rangle$. The obtained set of $\langle n_i \rangle$ enters an overdamped Langevin equation adapted from (6), which gives an updated distribution of $\{y_i\}$. We use the fourth-order Runge–Kutta method for the Langevin equation. The new distribution of $\{y_i\}$ is then inserted in equation (5). The iteration proceeds until a desired convergence is achieved, representing an adiabatic local minimum configuration both electronically and structurally.

Once a self-consistent solution for y_i is achieved, the total energy of the system is evaluated according to

$$E_{\text{tot}} = \sum_{n=1}^{N_e} E_n + \mathcal{H}_b, \quad (7)$$

where \mathcal{H}_b is given by equation (4). Comparison of the total energy is essential when more than one solution is found. We are especially interested in the local electronic properties, characterized by the electron local density of states (LDOS):

$$\rho_i(E) = \sum_n |\phi_i^n|^2 \delta(E - E_n). \quad (8)$$

This LDOS is proportional to the differential tunnelling conductance, which could be measured by, e.g., scanning tunnelling microscopy at low temperature.

We use the following parameter values, established by systematic comparison with thermodynamic data [27]: for the Morse potential $D_{GC} = 0.075$ eV, $a_{GC} = 6.9 \text{ \AA}^{-1}$ for a GC base-pair, and $D_{AT} = 0.05$ eV, $a_{AT} = 4.2 \text{ \AA}^{-1}$ for an AT pair; the spring constant $k_v = 0.025 \text{ eV \AA}^{-2}$, $\alpha = 0.35 \text{ \AA}^{-1}$; the electron hopping integral $t = 0.2$ eV and the on-site potential $\epsilon_i = 0.0$ eV for the AT base-pair and $\epsilon_i = -0.15$ for the CG base-pair. To ensure the validity of our adiabatic description, we consider the strong-coupling limit, $\alpha_v = 3.6 \text{ eV \AA}^{-1}$. The effect of the essential nonlinear inter-base-pair stacking interaction on the polaron structure is investigated by varying the parameter ρ . Two specific sequences are considered: the 68 homopolymer base-pair sequence with AAAAAA AAAAAAAAAA AAAAAAAAAA AAAAAAAAAA AAAAAAAAAA AAA and the 68 base-pair long viral P5 promoter sequence with GTGGC CATTAGGGT ATATATGGCC GAGTGAGCGA GCAGGATCTC CATTGACC GCGAAATTG AAC.

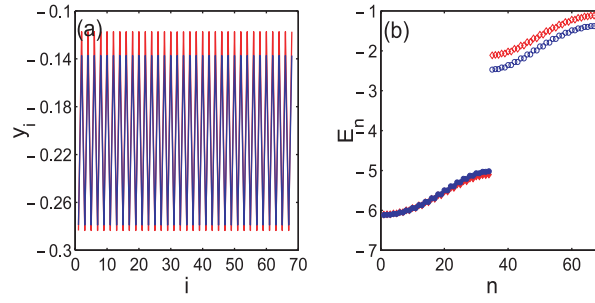


Figure 1. (a) Displacement field y_i , (b) electron eigenvalue spectrum E_n , for various values of $\rho = 0$ (red) and 8 (blue). The total electron number $N_e = 34$. The filled symbols in the right panel represent the occupied states.

Throughout the following discussion, the energy is measured in units of t and the displacement field in units of \AA . Periodic boundary conditions are used for simplicity.

Homopolymer sequence. In figure 1, we show, for the half-filled case ($N_e = 34$), the real space variation of the displacement field y_i and the electronic eigenvalue spectrum. Due to the strong coupling to the electronic degrees of freedom, the field y_i exhibits a bipartite behaviour (see figure 1(a)) in striking contrast to the non-coupling case, where the field is spatially constant. Correspondingly, the modulation of the displacement field with a period of two base-pairs causes the dimerization of the electronic state, i.e., a charge density wave state (not shown here). This electronic ordering results in the opening of an energy gap (see figure 1(b)). Increasing the amplitude of the nonlinear term ($\rho = 8$) reduces the modulation amplitude of the displacement field, which in turn reduces the gap amplitude. This indicates that the nonlinear term in the inter-base-pair coupling enhances the transfer probability of an electron at the Fermi energy. When an additional electron is doped into the half-filling background, the regular modulation of the displacement field collapses locally—a polaronic effect. For small amplitudes (e.g., $\rho = 0$ and 8) of the nonlinear term, the displacement field shows one dip at the collapse region, while for a large amplitude (e.g., $\rho = 16$), the collapse region is more spread out and two closely spaced dips appear. The two dips correspond to two spatial scales in the polaron—a smaller one induced by the nonlinearity from the electron–lattice coupling and a longer-range tail (which grows with ρ) from the nonlinear ‘elasticity’ coupling. For small values of ρ , the collapse region traps an intra-gap electronic state (i.e., the energy level is within the gap) and an ultra-band state (the energy level is outside the two bands). For a large value of ρ , the local collapse can trap two intra-gap states and two ultra-band states (see the right column of figure 2). *These small polaron effects arise from the strong coupling between the electron and lattice degrees of freedom.* In figure 3, we show the spatial variation of the electronic LDOS at the intra-gap energy levels. For small values of ρ , the LDOS peaks at the centre of the collapse region and sharply decays, indicating that the polaron state is tightly bound. In this range, the increase of ρ makes the peak width spread quantitatively, which is due to the narrowing of the gap. For a large value of ρ , the LDOS for each intra-gap polaronic state displays a double-peak structure at the collapse region. However, the structure within the double peaks is different between the two intra-gap states. This difference is reminiscent of the bonding and anti-bonding states in a quantum double-well system. Moreover, the finite range of these polaronic states is a direct measure of the range of the collapse region in the displacement field with two length scales, as noted above.

P5 promoter sequence. Because of the very different parameter values for the CG and AT base-pairs, the particular base-pair arrangement of this real viral sequence will clearly be

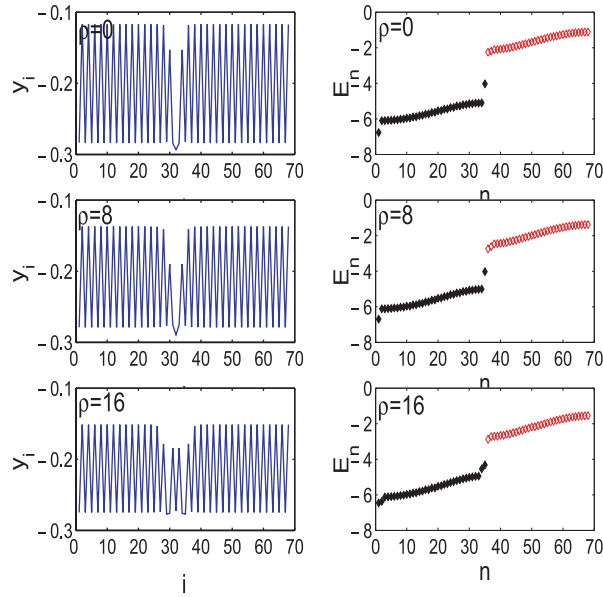


Figure 2. Displacement field y_i (left column) and electron eigenvalue spectrum E_n (right column) for $\rho = 0, 8, 16$. A single electron is doped into the half-filled background, i.e., $N_e = 35$. The intragap energy level $E_p = -4.03$ for $\rho = 0$ and -4.03 for $\rho = 8$, and $E_{pa} = -4.54$ and $E_{pb} = -4.32$ for $\rho = 16$. The filled symbols in the right panels represent the occupied states.

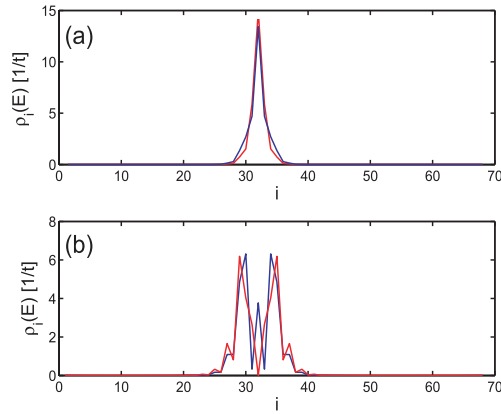


Figure 3. The LDOS at E_p for $\rho = 0$ (red curve) and $\rho = 8$ (blue curve) (a), and at E_{pa} (red curve) and E_{pb} (blue curve) for $\rho = 16$ (b). The other parameter values are the same as in figure 2.

very important in determining the spatial distribution of the displacement field. In particular, the polaronic length scales now have to adjust to (and potentially compete with) the base-pair sequence ‘disorder’, which can itself produce localized states. As shown in figure 4, we find that the segments with a sequence like TATATAT (sites 15–21)¹ are stretched, though not fully, while those with a sequence like GGCC (sites 22–25) are pinned close to the equilibrium positions (i.e., $y_i = 0$). The segment between the sites 26 and 53 has an oscillation in y_i due to the alternative arrangement of C-G and A-T base-pairs. The rich behaviour of the

¹ Note that, for simplicity, we have taken the parameter values for A and T bases or C and G bases to be identical.

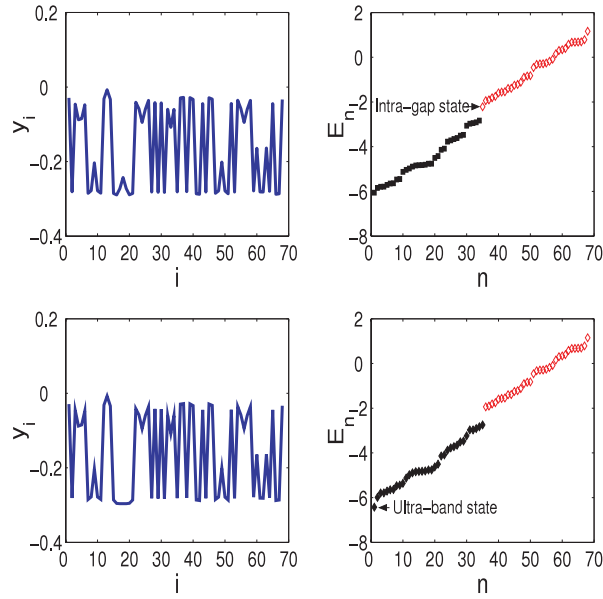


Figure 4. Spatial variation of the displacement field y_i (left column) and electron eigenvalue spectrum E_n (right column) for $\rho = 8$. The upper panels are for the half-filled case $N_e = 34$ and the lower ones for the case of one electron doped into the half-filled background, i.e., $N_e = 35$. The filled symbols in the right panels represent the occupied states.

spatial variation of the base-pair displacement field originates from the interplay of the strong electron–lattice coupling and the unique coloured ‘disorder’ sequence of a typical DNA chain (e.g., the P5 promoter considered here). In addition, the various segments with equivalent base-pair sequences manifest various minibands in the electronic energy spectrum (see the right column of figure 4). The gap opened reflects the modulation of y_i (correspondingly the electron density n_i) in the segment between sites 26 and 53. Compared to the homopolymer sequence, the gap is much diminished in the heterogeneous P5 promoter sequence. (Indeed the gap can be completely suppressed in a real sequence with even stronger randomness.) The incompletely stretched region around the 18th site traps an intra-gap state (marked in the upper right panel of figure 4). We emphasize that this state exists in the half-filled case. It is highly localized, showing an extremely narrow peak in the LDOS (see figure 5(a)). When one more electron is added to the half-filled background, the base-pair at the 18th site stretches completely (i.e., reaches the maximum) so that the pre-existing localized state in the half-filled case is completely compensated by the appearance of an ultra-band state (marked by in the right lower right panel of figure 4). This shows that the detailed lattice structure is very sensitive to the number of electrons in the system. In figure 5(b), we have also shown the LDOS at the ultra-band state energy for the one-electron doping case. It is localized at the same position as the intra-gap state in the half-filling case. This one-to-one correspondence provide an accurate spatial location of the change in the lattice dynamics upon electron doping. Experimentally, the STM technique should be useful in studying the predicted features.

In conclusion, we have studied self-consistently, in an adiabatic regime, the local base-pair and electronic structure in the PBH model of DNA. Both homopolymer and realistic viral P5 promoter sequences have been considered. In the homopolymer sequence, a dimerized state is formed at electronic half-filling (i.e., one ‘spinless’ electron per two sites), while a

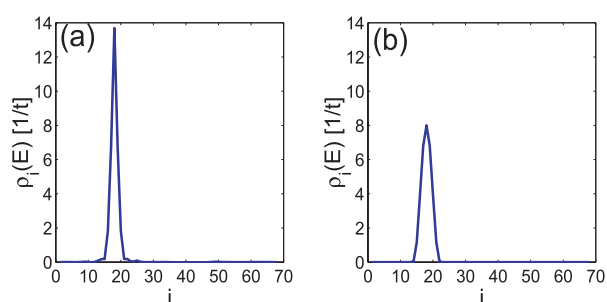


Figure 5. The LDOS at the intra-gap bound state energy $E_{\text{intra}} = -2.21$ (a) for the half-filled case, and at the ultra-band state energy $E_{\text{ultra}} = -6.43$ (b) for the case of one doped electron.

localized polaron state is induced by adding one electron (or hole). Notably, increasing the nonlinear inter-base-pair stacking interaction can qualitatively change the local structure of the polaron, including introduction of two characteristic length scales. Significantly, for the viral P5 promoter sequence, at half filling, an intra-gap bound state can be formed due to the specific ‘disorder’ arrangement of base-pairs in this sequence. A real space imaging of the local density of states locates the bound state. Doping an electron into this half-filled background can annihilate the bound state.

Acknowledgments

We thank G Kalosakas for valuable discussion. We also gratefully acknowledge Professor A Usheva for helpful discussions regarding the P5 promoter. This work was supported by the US Department of Energy.

References

- [1] Bixon M and Jortner J 1999 *Adv. Chem. Phys.* **106** 35
- [2] Porath D, Cuniberti G and Felice R D 2004 *Top. Curr. Chem.* **237** 183
- [3] Endres R G, Cox D L and Singh R R P 2004 *Rev. Mod. Phys.* **76** 195
- [4] Stemp E D A, Arkin M R and Barton J K 1997 *J. Am. Chem. Soc.* **119** 2921
- [5] Breslin D T, Coury J E, Anderson J R, MacFail-Isom L, Kan Y, Williams L D, Bottomley L A and Schuster G B 1997 *J. Am. Chem. Soc.* **119** 5043
- Schuster G B 2000 *Acc. Chem. Res.* **33** 253
- [6] Kelley S O, Jackson N M, Hill M G and Barton J K 1999 *Angew. Chem.* **104** 443
- [7] Storhoff J J and Mirkin C A 1999 *Chem. Rev.* **99** 1849
- [8] Conwell E M and Rakhmanova S V 2000 *Proc. Natl Acad. Sci. USA* **87** 4556
- Rakhmanova S V and Conwell E M 2001 *J. Phys. Chem. B* **105** 2056
- [9] Basko D M and Conwell E M 2002 *Phys. Rev. E* **65** 061902
- [10] Hennig D 2002 *Eur. Phys. J. B* **30** 211
- [11] Komineas S, Kalosakas G and Bishop A R 2002 *Phys. Rev. E* **65** 061905
- [12] Alexandre S S, Artacho E, Soler J M and Chacham H 2003 *Phys. Rev. Lett.* **91** 108105
- [13] Kalosakas G, Rasmussen K Ø and Bishop A R 2003 *J. Chem. Phys.* **118** 3731
- Kalosakas G, Rasmussen K Ø and Bishop A R 2004 *Synth. Met.* **141** 93
- [14] Maniadis P, Kalosakas G, Rasmussen K Ø and Bishop A R 2003 *Phys. Rev. B* **68** 174304
- [15] Chang C-M, Castro Neto A H and Bishop A R 2004 *Chem. Phys.* **303** 189
- [16] Yoo K-H, Ha D H, Lee J-O, Park J W, Kim J, Kim J J, Lee H-Y, Kawaim T and Choi H Y 2001 *Phys. Rev. Lett.* **87** 198102
- [17] Peyrard M and Bishop A R 1989 *Phys. Rev. Lett.* **62** 2755
- [18] Dauxois T, Peyrard M and Bishop A R 1993 *Phys. Rev. E* **47** R44

- [19] Choi C H, Kalosakas G, Rasmussen K Ø, Bishop A R and Usheva A 2004 *Nucleic Acids Res.* **32** 1584
- [20] Ares S, Voulgarakis N K, Rasmussen K Ø and Bishop A R 2005 *Phys. Rev. Lett.* **94** 035504
- [21] Roche S 2003 *Phys. Rev. Lett.* **91** 108101
- [22] Roche S, Bicout D, Maciá E and Kats E 2003 *Phys. Rev. Lett.* **91** 228101
- [23] Tanaka H and Kawai T 2006 *Surf. Sci.* **539** L531
- [24] Dauxois T and Peyrard M 1995 *Phys. Rev. E* **51** 4027
- [25] Campa A and Giansanti A 1998 *Phys. Rev. E* **58** 3585
- [26] Cule D and Hwa T 1997 *Phys. Rev. Lett.* **79** 2375
- [27] Campa A and Giansanti A 1998 *Phys. Rev. E* **58** 3585